

Journal of Materials Chemistry C

Accepted Manuscript



This is an *Accepted Manuscript*, which has been through the Royal Society of Chemistry peer review process and has been accepted for publication.

Accepted Manuscripts are published online shortly after acceptance, before technical editing, formatting and proof reading. Using this free service, authors can make their results available to the community, in citable form, before we publish the edited article. We will replace this *Accepted Manuscript* with the edited and formatted *Advance Article* as soon as it is available.

You can find more information about *Accepted Manuscripts* in the [Information for Authors](#).

Please note that technical editing may introduce minor changes to the text and/or graphics, which may alter content. The journal's standard [Terms & Conditions](#) and the [Ethical guidelines](#) still apply. In no event shall the Royal Society of Chemistry be held responsible for any errors or omissions in this *Accepted Manuscript* or any consequences arising from the use of any information it contains.

Cite this: DOI: 10.1039/c0xx00000x

www.rsc.org/xxxxxx

ARTICLE TYPE

Novel hole transport materials based on *N,N'*-disubstituted-dihydrophenazine derivatives for electroluminescent diodes

Zhiwen Zheng^a, Qingchen Dong^b, Liao Gou^a, Jian-Hua Su^{*a} and Jinhai Huang^{*a}

Received (in XXX, XXX) XthXXXXXXXXXX 20XX, Accepted Xth XXXXXXXXXXXX 20XX

DOI: 10.1039/b000000x

A series of novel hole transport materials for organic light-emitting diodes (OLEDs) based on 9,14-diphenyl-9,14-dihydrodibenzo[a,c]phenazine were synthesized and characterized by ¹H NMR and ¹³C NMR, mass spectrometry and single crystal structure analysis methodology. The crystal structures of three selected molecules reveal large dihedral angles between different functional units. The electro-optical properties of the materials were examined by UV-Vis absorption, photoluminescence spectroscopy and cyclic voltammetry. The HOMO of the materials were between 4.83-5.08 eV, indicating a good match between the HOMO of indium tin oxide (ITO) and the HOMO of light-emitting layer, which render the promising candidates as hole transport materials for organic light-emitting devices. In terms of the device with the structure of ITO/HTM (60 nm)/Alq₃ (50 nm)/LiF (1 nm)/Al (200 nm), the device **b** using *N,N*-diphenyl-4'-(14-phenyldibenzo[a,c]phenazin-9(14H)-yl)-[1,1'-biphenyl]-4-amine presented a maximum luminance of 17437 cd/m² at 10.7 V and kept a high current efficiency (the maximum current efficiency is 2.25 cd/A) at a high current density (> 500 mA/cm²), which illustrates the exploited material possesses good hole transport and stable properties.

Introduction

Organic light-emitting diodes (OLEDs) have attracted wide attention from academic to industry, because of its high brightness, quick response, large viewing angle, simple manufacture process and flexibility, etc.¹⁻³ Its commercial applications in mobile phones and full-color display have made progress since the pioneering work of Tang.⁴

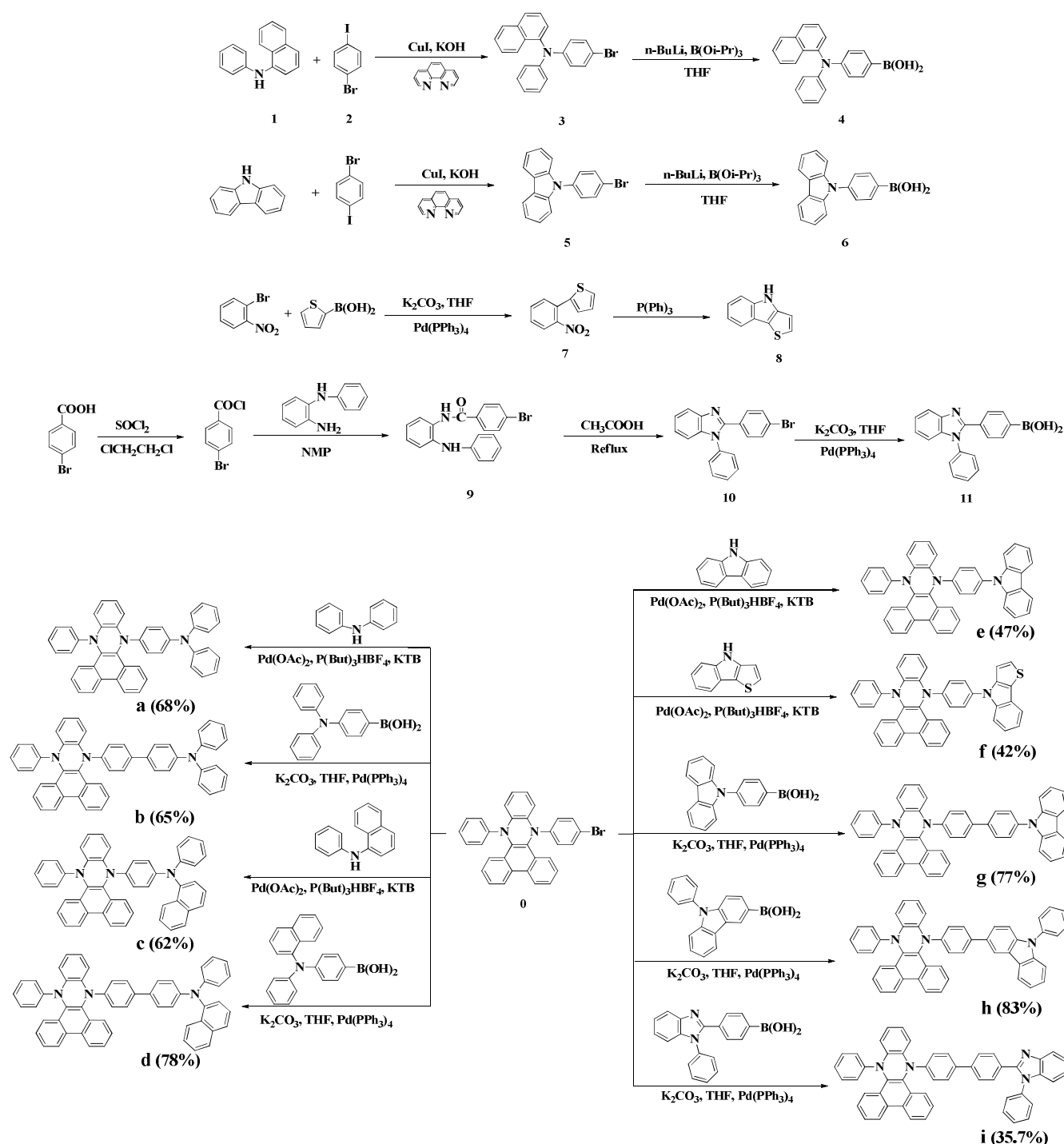
Typical multilayered OLEDs consist of a transparent anode (like an indium tin oxide (ITO) glass substrate), a hole transport material (HTM), a light emitting layer and electron transport material (tris(8-quinolinolato) aluminium(III) (Alq₃)) and a metallic cathode.⁴ To achieve a good quality of OLEDs with high efficiency, many efforts have been carried out on hole transport layer (HTLs) as the hole transport materials will decrease the energy barrier between the anode and organic emitter.⁵⁻⁷ Generally, a useful hole transport material for electroluminescence diodes should possess good hole mobility, morphologically stable thin films, an appropriate HOMO level to ensure a low energy barrier for hole injection from the anode into the emissive layer, and a suitable LUMO level to block electron injection from the EML to the HTL.⁵

Traditionally, the molecular structures of hole transport materials contain electron-donating moieties (such as diphenylamine, carbazole etc), owing to its attractive properties of high charge carrier mobility and low ionization potentials. So far, a large number of aromatic amine derivatives have been utilized for the effective HTLs, including diamine TCTA⁴,

N,N,N',N'-tetraphenylbenzidine family such as TPD⁸ and NPB⁹, Shirota's starburst molecules with various cores¹⁰ and shells¹¹, linear oligomeric amines¹², spiro-linked or spirocyclicbenzidines¹³ and so on.

4,4'-bis[*N*-(1-naphthyl)-*N*-phenylamino] biphenyl (NPB) is considered as one of the most widely used hole transport materials owing to its good carrier mobility (8.8×10⁻⁴ cm² V⁻¹), high transparency for visible light and well matched HOMO level (5.4 eV) for hole injection and hole transport.⁴ However, many research groups are still looking for some alternative materials to facilitate the formation of thermally and morphologically stable amorphous films.¹⁴⁻¹⁸ For example, 5,10-diaryldihydrophenazines have been reported and used in OLEDs.¹⁹

In this work, a series of novel asymmetrically substituted 5,10-diaryl-5,10-dihydrophenazines as hole transport materials with high efficiency and thermal stability for OLEDs were designed and synthesized. To improve the hole transfer characteristic and achieve high thermal stability, phenathrene unit was introduced. The *N,N'*-positions were substituted with phenyl and bulky aromatic amine groups to obtain asymmetrical structure for pursuing amorphous morphology.²⁰⁻²² Moreover, the introduction of aromatic amine groups can effectively modify the HOMO levels and improve the hole mobility. The derivatives were characterized by ¹H NMR, ¹³C NMR, ESI-MS, single crystal structure analysis methodologies and UV-Vis spectroscopy. Meanwhile, some of the synthesized materials were used to fabricate organic light emitting devices to test their hole transport performance.



Scheme 1 Synthetic route to the desired compounds.

Results and discussion

5 Synthesis and Characterization

The synthetic route to these target compounds was depicted in **Scheme 1**. Firstly, the starting materials **0-2** were obtained from the commercial resource. The other intermediates **3-11** were synthesized from previous reports with a high yield, and the more synthetic details were described in the **Electronic Supplementary Information (ESI)**.²⁴⁻²⁹ The purification of

intermediates was commonly performed by flash column chromatography and recrystallization. These targeted compounds were synthesized by traditional organic name reactions such as Suzuki or Buchwald-Hartwig cross coupling reaction of the starting material **0** and relative intermediates, which were given as pure powders with yields from 35% to 85%. Good solubility of these target compounds facilitates their purification procedure. Repeated temperature-gradient vacuum sublimation was required for further purification of these materials when used in OLEDs. All these new compounds were characterized fully by ^1H NMR

and ^{13}C NMR and mass spectrometry.

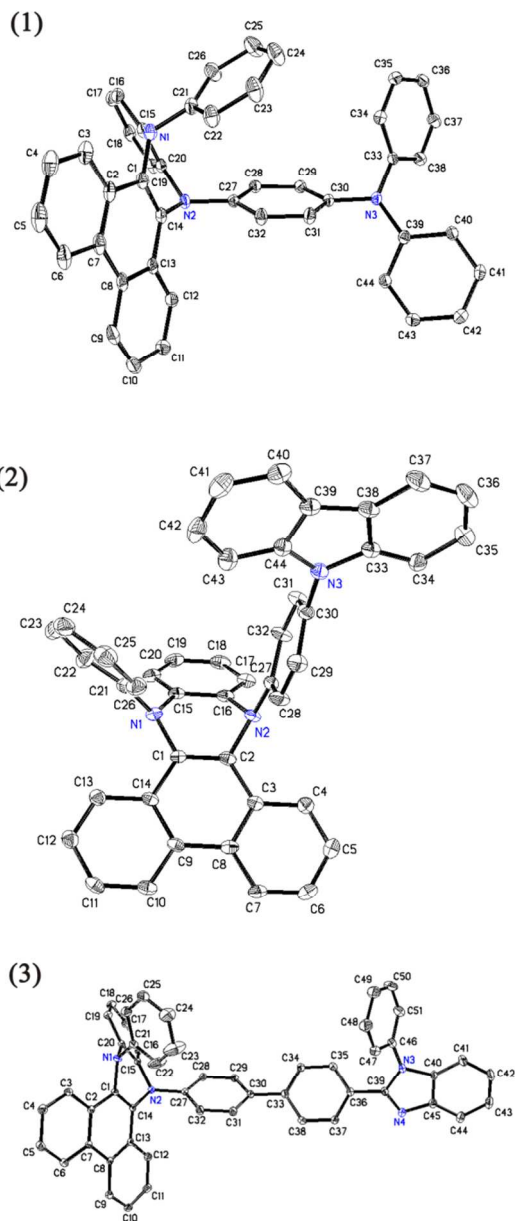


Figure 1 Single crystal structure of selected compounds: 1) a; 2) e; 3) i.

X-Ray crystal structure

In order to look at the conformation of these compounds, the crystal structures of **a**, **e** and **i** were determined. Single crystals of compounds **a**, **e** and **i** were obtained by crystallization from $\text{CH}_2\text{Cl}_2/n\text{-hexane}$. The molecular structures were given in **Figure 1** and their packing arrangements were shown in **Electronic Supplementary Information (ESI)**. In compound **a**, it is shown that $\text{C}(21)\text{-N}(1)\text{-C}(1)$, $\text{C}(21)\text{-N}(1)\text{-C}(15)$ and $\text{C}(1)\text{-N}(1)\text{-C}(15)$ are 117.48° , 116.92° and 109.93° , respectively. In carbazole group of compound **e**, $\text{C}(44)\text{-N}(3)\text{-C}(33)$, $\text{C}(44)\text{-N}(3)\text{-C}(30)$, $\text{C}(33)\text{-N}(3)\text{-C}(30)$ are 109.2° , 123.9° , 126.8° , respectively. The dihedral angle between the 9,14-diphenyl-9,14-dihydrodibenzo[a,c]phenazine ring and carbazole group is 78.5° . In terms of compound **i**, the dihedral angle between the 9,14-diphenyl-9,14-

dihydrodibenzo[a,c]phenazine ring and 1,2-diphenyl-1H-benzo[d]imidazole group is 136.6° . These large angles are useful to decrease the intermolecular $\pi\text{-}\pi$ interaction and favour amorphous morphology.

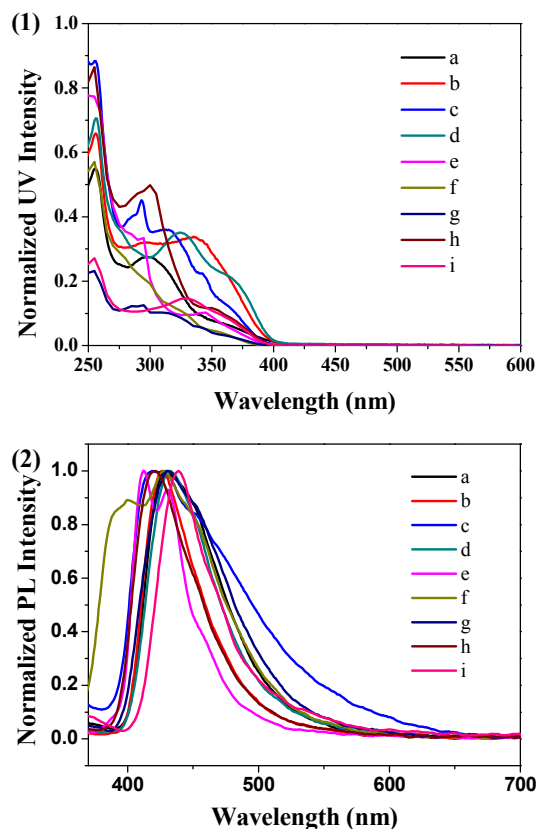


Figure 2 1) UV-Vis absorption spectra of all compounds in cyclohexane and 2) fluorescence spectra of all compounds in solid state.

Optical property

The optical properties of these compounds **a-i** were investigated in both solid-state and solvent. It was depicted in **Figure 2** and the pertinent data were summarized in **Table 1**. **Figure 2 (1)** showed that the absorption bands were observed around 250-350 nm, which can be attributed to $\pi\text{-}\pi^*$ transitions of the conjugated aromatic segment. The PL studies in solid state (**Figure 2 (2)**) were performed to examine the emission in the condensed phase. PL spectra indicated that compounds **a-h** in solid phase behaved two maximum emission bands at 402-433 nm and 430-455 nm while compound **i** contained only one maximum emission band located at 438 nm, implying the slight influence based on different *N*-substituted structure between the electron-donating group and electron-deficient group. Overall, the little difference of the spectra of **a-h** attributes to the large dihedral angles between the phenazine core and substituent, which is in agreement with their crystal structures.

Solvent effect was usually observed in the structure of *N,N'*-disubstituted-dihydrophenazine framework. To determine the solvent effect of these compounds, compound **a** was investigated in different solutions by increasing the solvent polarity including tetrahydrofuran (THF), dichloromethane (DCM), ethanol (EtOH), acetonitrile (MeCN), *N,N*-dimethylformamide (DMF). The

emission spectra of **a** was described in **Figure 3**. As shown in **Figure 3**, compound **a** exhibited a slight emission spectral change when the polarity of solvents increased. The emission peak at 507 nm in THF was shifted to 545 nm in DMF. The phenomenon reveals the good solvent stabilization of the excited state between these dihydrophenazine derivatives and the polar solvents. Moreover, The PL spectra in different solvent of compound **a** showed large red-shifted compared with that in thin film, implying that no significant intermolecular interaction occurred in the solid state.⁶

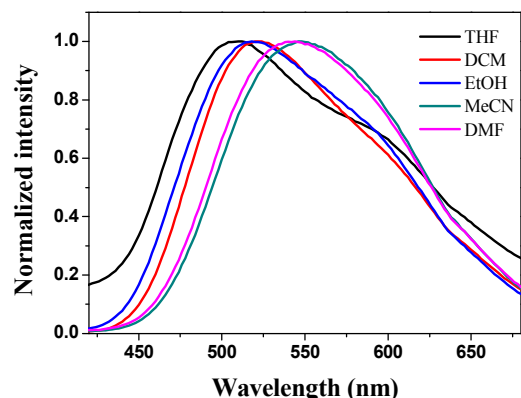


Figure 3 Solvent effect of compound **a**

Electrochemistry

The electrochemical behaviours of derivatives based on 9,14-diphenyl-9,14-dihydrodibenzo[*a,c*]phenazine were examined by cyclic voltammetry (CV) using a standard three-electrode electrochemical cell in an electrolyte solution (0.1M TBAPF₆/DCM), tetrabutylammonium hexafluorophosphate as the electrolyte and ferrocene as external reference. The working electrode was glassy carbon, the counter electrode was a platinum wire, and the reference electrode was SCE. Some selected data were shown in **Figure 4** (others see **ESI**) and all the results were summarized in **Table 1**. The HOMO and LUMO energy levels of these compounds were calculated from the onset potentials of oxidation and their absorption spectra. The CV curves of these materials with a multi-reversible electron oxidation are attributable to the aromatic amine and dihydrophenazines. As we can see that the HOMO levels of all compounds were calculated to range from -4.83 to -5.08 eV and LUMO levels were from -1.60 to -1.85 eV. Accordingly, the optical band gaps (E_g) were determined nearly 3.25 eV. This indicates that the *N,N'*-disubstituted-dihydrophenazine framework could enhance the HOMO level, and thereby enhance the hole affinity and hole

injection ability of the conjugated phenazine derivatives. Besides, the high HOMO energy level indicates that the *N,N'*-disubstituted-dihydrophenazine framework could rationally be used as hole transport and injection materials in OLEDs.

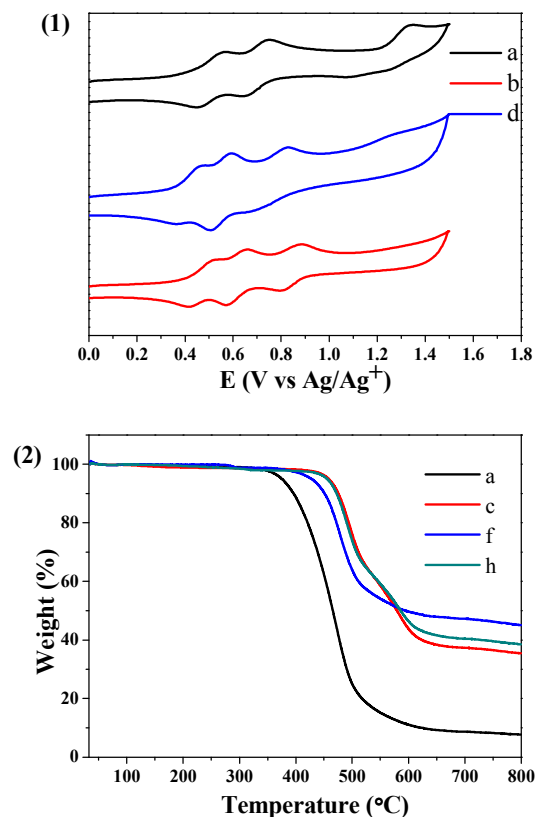


Figure 4 Electrochemistry and TGA of some target molecules: 1) electrochemistry of **a**, **b** and **d**; 2) TGA of **a**, **c**, **f** and **h**.

Thermal properties

Thermogravimetric analysis (TGA) was employed to investigate the thermal properties of **a-i**, the related data were listed in **Table 1** and some were shown in **Figure 4** (the rest data please see **ESI**). TGA measurements showed that all compounds exhibited high decomposition temperatures (T_d , 5% weight loss) from 375 to 463 °C, which indicates **a-i** have good thermal ability. **Figure 4** showed that the stability is in accordance with the molecular weight. No doubt that those materials are stable enough to be fabricated into devices by vacuum thermal evaporation technology, which can improve the film morphology, reduce the possibility of phase separation upon heating and prolong the life time of the devices.

Table 1 Optical and electrochemical properties of all compounds.

	$\lambda_{\text{abs}}(\text{nm})^a$	$\lambda_{\text{em}}(\text{nm})^b$	HOMO(eV) ^c	LUMO(eV) ^c	$E_g(\text{eV})^d$	$T_d(\text{°C})$
a	256/298/366	428/450	-4.83	-1.60	3.23	375
b	256/297/335	427/454	-4.89	-1.64	3.25	460
c	255/292/314	424/455	-4.87	-1.65	3.22	458
d	257/325/371	433/454	-4.87	-1.75	3.12	441
e	252/296/344	413/430	-4.92	-1.70	3.21	463
f	253/353	402/430	-5.08	-1.80	3.27	428
g	255/294/317	431/455	-5.07	-1.85	3.22	443
h	255/302/352	420/451	-5.06	-1.86	3.20	455
i	255/330	438	-4.92	-1.71	3.21	456

^aMeasured in cyclohexane. ^bMeasured in solid state. ^cMeasured versus Fc/Fc⁺ in CH₂Cl₂. LUMO energy was estimated based on the HOMO levels and E_g . ^dDetermined from the absorption threshold.

EL performance

In order to further study their charge transport properties, OLED devices with ITO/HTM (60 nm)/Alq₃ (50 nm)/LiF (1 nm)/Al (200 nm) were fabricated with using **b**, **g** as the hole transport layer and Alq₃ as the emit layer and electron transport layers, LiF and Al as the electron inject layer and cathode, respectively. It was depicted in **Figure 5**. For comparison, the typical double layer device with the configuration of ITO/NPB (60 nm)/Alq₃ (50 nm)/LiF (1 nm)/Al (200 nm) was also fabricated. Their device performance results were summarized in **Table 2**.

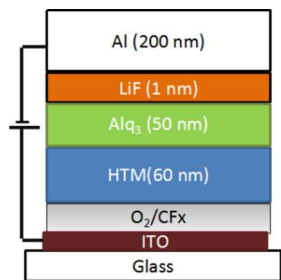


Figure 5 Structure of the device

The current density-voltage-luminance (I-V-L) characteristics of the devices with various hole transport materials were displayed in **Figure 6**. The current density and luminance of device **b** and device **g** were comparable to the device based on **NPB** at the same driving voltage. Moreover, the device **b** achieved a maximum luminance of 17437 cd/m² at 10.7 V.

The current efficiencies of the devices were revealed in **Figure 6**. The devices based on the new hole transport materials had better current efficiency than the **NPB**-based device. The maximum current efficiency for devices were 2.25, 1.98 and 2.0 cd/A, respectively. It showed that the current density and luminance based device **b** and **g** are lower than them based **NPB** at the same driving Voltage. This indicates that the devices based on the phenazines can more effectively balance the hole and electron in emitting layer. Meanwhile, all the devices also kept a high current efficiency at a high current density (> 500 mA/cm²), which illustrates the exploited materials possesses good hole transport and stable properties.

Figure 6 (3) showed that the EL spectra of device **b** and **g** at 10 voltages. These spectra exhibited the peak wavelength at about 536 nm, which is similar to the Alq₃ emission, indicating that the emissions originate from the emitting layer (Alq₃ layer). This also suggests these compounds have good hole mobility and can effectively transport the hole into the emitting layer.

Conclusions

In summary, a series of new hole transport materials based on *N,N'*-disubstituted-dihydrophenazine framework were designed and synthesized for OLEDs' application. It has shown that both the structure and electrochemistry property of these derivatives

render them as promising candidates used in HTMs. The **b**-based device offered the highest efficiency of 2.25 cd/A with turn-on voltage of 4.35 V, which was superior to that of **NPB**-based device in the same condition. Owing to the better thermal stability and the higher performance of **b**-based device, it is a promising hole transport material to be applied in OLEDs.

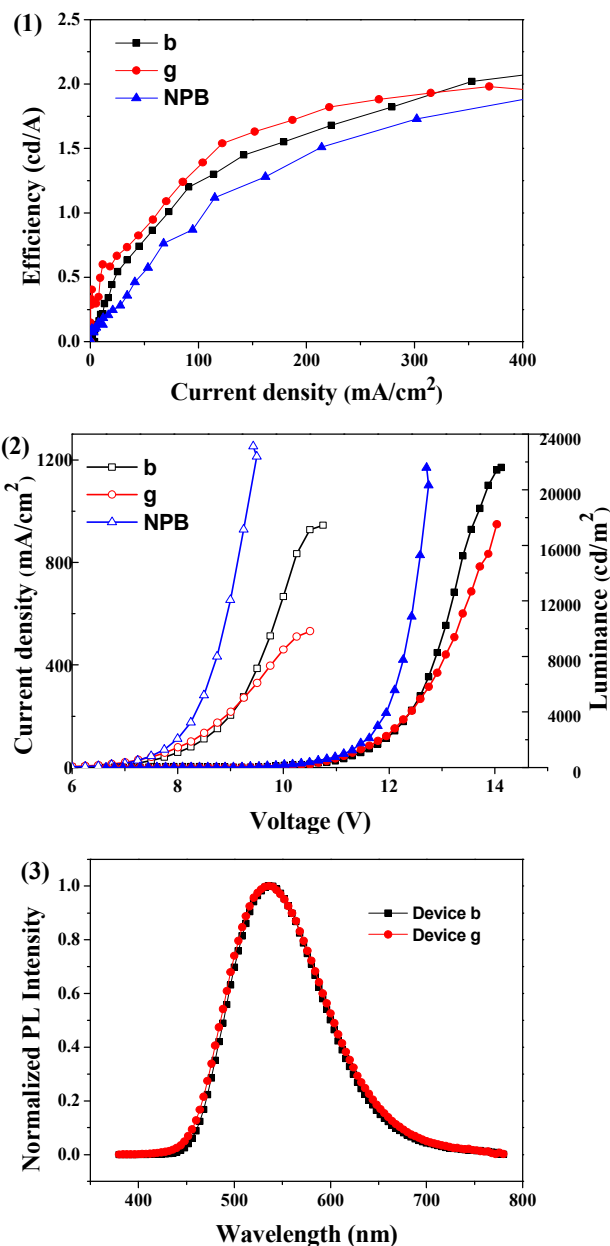


Figure 6 1) EL efficiencies of device **b**, **g**, **NPB**; 2) Current density-voltage-luminance characteristic of device **b**, **g**, **NPB**; 3) EL spectra of device **b** and **g** at 10 V

Table 2 EL performances of device **NPB**, **b** and **g**.

Device	Turn-on voltage(V)	Max brightness(cd m ⁻²)	Current efficiency(cd A ⁻¹)	$\lambda_{em}(nm)$	CIE _(x,y)
NPB	3.88	22946	2.0	536	(0.35,0.54)
b	4.35	17437	2.25	537	(0.35,0.54)
g	4.19	9794	1.98	536	(0.36,0.53)

Experimental

General and Synthesis

¹H NMR and ¹³C NMR spectra were recorded on Bruker AM 400 spectrometer at room temperature. Mass spectra were recorded on Waters LCT Premier XE spectrometer. Ultraviolet - visible (UV-Vis) absorption spectra were recorded on a Varian Cary 500 spectrophotometer. Photoluminescence (PL) spectra were recorded on Varian-Cary fluorescence spectrophotometer. The cyclic voltammograms of the products were determined with a Versastat II electrochemical workstation (Princeton applied research) using a normal three-electrode cell with a Pt working electrode, a Pt wire counter electrode, and a regular calomel reference electrode in saturated KCl solution, 0.1 M tetrabutylammonium hexafluorophosphate (TBAPF₆) used as the supporting electrolyte in dichloromethane solution. Thermogravimetric analysis (TGA) was measured by using DMA2980/DS at a heating rate of 10 °C/min under nitrogen.

N,N-diphenyl-4-(14-phenyldibenzo[a,c]phenazin-9(14H)-

yl)aniline (a): Tri-tert-butylphosphinetetrafluoroborate (5.8 mg) and palladiumacetate (4.5 mg) were dissolved in methylbenzene in 50 mL one-necked round-bottomed flask. The mixture was stirred under nitrogen atmosphere. After 15 minutes, diphenylamine (0.3g, 1.7 mmol), 9-(4-bromophenyl)-14-phenyl-9,14-dihydrodibenzo[a,c]phenazine (0.3 g, 1.7 mmol), potassiumtert-butoxide (0.224 g, 2.0 mmol) were added and heated to 120 °C. After 20 h, the mixture was cooled to room temperature and filtered. The filtrate was washed with water and dried with MgSO₄. The solvent was evaporated in vacuo and the residue was purified by flash column chromatography (petroleum ether: dichloromethane =10:1) and recrystallization (methylbenzene) to get pure product. Light yellow powder; yield: 0.41 g (68%). ¹H NMR (400 MHz, CDCl₃) δ: 8.76 (d, *J* = 8.2 Hz, 2H), 8.30 (d, *J* = 8.0 Hz, 1H), 8.20 (d, *J* = 8.1 Hz, 1H), 7.82 – 7.76 (m, 1H), 7.74 – 7.56 (m, 5H), 7.37 (dd, *J* = 9.3, 5.6 Hz, 2H), 7.16 (t, *J* = 7.8 Hz, 4H), 7.07 (t, *J* = 7.9 Hz, 2H), 6.90 (m, 11H), 6.76 (d, *J* = 9.0 Hz, 2H). ¹³C NMR (100 MHz, CDCl₃) δ 148.10, 148.08, 147.87, 145.55, 145.06, 144.75, 141.28, 138.97, 138.26, 129.81, 129.58, 128.95, 128.69, 127.64, 127.19, 127.06, 126.57, 126.02, 125.60, 125.45, 124.52, 122.97, 121.82, 120.91, 118.52, 116.80. HRMS (ESI, *m/z*): [M+H]⁺ calcd for C₄₄H₃₂N₃, 602.2596; found, 602.2596.

N,N-diphenyl-4'-(14-phenyldibenzo[a,c]phenazin-9(14H)-yl)-

[1,1'-biphenyl]-4-amine (b): A mixed solution of 9-(4-bromophenyl)-14-phenyl-9,14-dihydrodibenzo[a,c]phenazine (0.5 g, 0.97 mmol), 4-(Diphenylamino)phenylboronic acid (0.3 g, 1mmol), tetrakis(triphenylphosphine)palladium(0) (0.1 g, 0.086mmol), toluene (20 mL) and 2 N K₂CO₃ aqueous solution (5 mL) was heated at 100 °C with stirring under an argon atmosphere. After 12 h, the mixture was cooled to room temperature. Then the mixture was quenched with water (20 mL) and extracted with CH₂Cl₂ (3×50 mL). The combined organic phase was dried (anhydrous MgSO₄). The solvent was removed in vacuo and the residue was purified by flash column chromatography (petroleum ether: dichloromethane =10:1) and recrystallized (methylbenzene) to give pure product. White

powder; yield: 0.44 g (65%); ¹H NMR (400 MHz, CDCl₃) δ: 8.74 (d, *J* = 8.0 Hz, 2H), 8.13 (t, *J* = 7.2 Hz, 2H), 7.76 (s, 2H), 7.64 (s, 2H), 7.54 (d, *J* = 5.7 Hz, 2H), 7.35 (s, 2H), 7.30 (d, *J* = 8.5 Hz, 2H), 7.22 (t, *J* = 7.8 Hz, 6H), 7.14 – 6.94 (m, 15H), 6.78 (s, 1H). ¹³C NMR (100 MHz, CDCl₃) δ 147.75, 147.67, 146.67, 146.46, 144.80, 144.69, 138.12, 137.92, 134.80, 133.11, 129.93, 129.46, 129.40, 129.23, 129.08, 128.84, 128.27, 127.38, 127.30, 127.07, 127.03, 126.89, 126.56, 125.44, 125.42, 125.34, 124.64, 124.19, 123.07, 122.71, 121.16, 117.00, 116.88. HRMS (ESI, *m/z*): [M+H]⁺ calcd for C₅₀H₃₆N₃, 678.2909; found, 678.2969.

N-phenyl-*N*-(4-(14-phenyldibenzo[a,c]phenazin-9(14H)-

yl)phenyl)naphthalen-1-amine (c): White powder yield: 0.4 g (62%). ¹H NMR (400 MHz, CDCl₃) δ: 8.70 (d, *J* = 8.2 Hz, 2H), 8.20 (d, *J* = 8.1 Hz, 1H), 8.14 (d, *J* = 7.9 Hz, 1H), 7.81 (s, 1H), 7.79 (d, *J* = 2.7 Hz, 1H), 7.71 (d, *J* = 6.8 Hz, 1H), 7.65 (dd, *J* = 13.0, 8.0 Hz, 4H), 7.54 (dd, *J* = 15.3, 7.6 Hz, 2H), 7.42 – 7.38 (m, 1H), 7.36 (d, *J* = 8.0 Hz, 1H), 7.28 (d, *J* = 5.8 Hz, 2H), 7.24 (s, 1H), 7.13 (d, *J* = 6.8 Hz, 1H), 7.08 – 6.99 (m, 4H), 6.92 (d, *J* = 8.1 Hz, 2H), 6.82 (dd, *J* = 17.0, 8.4 Hz, 4H), 6.74 (dd, *J* = 16.4, 7.6 Hz, 4H). ¹³C NMR (100 MHz, CDCl₃) δ 139.84, 129.01, 128.91, 128.72, 127.82, 126.65, 126.46, 126.37, 126.32, 126.19, 126.06, 125.62, 124.86, 124.60, 124.39, 123.65, 123.54, 122.29, 122.09, 120.19, 119.24, 118.82, 115.92, 115.63, 108.80. HRMS (ESI, *m/z*): [M+H]⁺ calcd for C₄₈H₃₄N₃, 652.2753; found, 652.2750.

N-phenyl-*N*-(4'-(14-phenyldibenzo[a,c]phenazin-9(14H)-yl)-

[1,1'-biphenyl]-4-yl)naphthalen-1-amine (d): White powder; yield: 0.57 g (78%). ¹H NMR (400 MHz, CDCl₃) δ: 8.77 (d, *J* = 8.2 Hz, 2H), 8.18 – 8.11 (m, 2H), 7.93 (d, *J* = 8.5 Hz, 1H), 7.89 (d, *J* = 8.0 Hz, 1H), 7.78 (dd, *J* = 8.6, 6.0 Hz, 3H), 7.67 (t, *J* = 7.6 Hz, 2H), 7.60 – 7.54 (m, 2H), 7.48 (d, *J* = 7.4 Hz, 1H), 7.46 – 7.43 (m, 1H), 7.39 – 7.31 (m, 4H), 7.30 – 7.30 (m, 3H), 7.25 – 7.17 (m, 4H), 7.08 – 6.96 (m, 10H), 6.94 (t, *J* = 7.3 Hz, 1H), 6.80 (t, *J* = 6.5 Hz, 1H). ¹³C NMR (100 MHz, CDCl₃) δ 148.34, 147.68, 147.11, 146.53, 144.76, 144.71, 143.45, 138.06, 137.94, 137.91, 135.26, 133.73, 133.20, 131.23, 129.90, 129.69, 129.45, 129.39, 129.09, 129.07, 128.81, 128.38, 128.26, 127.36, 127.24, 127.22, 127.00, 126.93, 126.77, 126.52, 126.46, 126.41, 126.36, 126.14, 125.39, 125.33, 124.62, 124.61, 124.27, 123.03, 121.91, 121.86, 121.66, 121.13, 120.29, 117.04, 116.84, 115.29, 113.62. HRMS (ESI, *m/z*): [M+H]⁺ calcd for C₅₄H₃₈N₃, 728.3066; found, 728.3063.

9-(4-(9H-carbazol-9-yl)phenyl)-14-phenyl-9,14-

dihydrodibenzo[a,c]phenazine (e): White powder; yield: 0.28 g (47%); ¹H NMR (400 MHz, CDCl₃) δ: 8.84 – 8.77 (m, 2H), 8.39 – 8.34 (m, 1H), 8.21 (d, *J* = 8.1 Hz, 1H), 8.10 (d, *J* = 7.6 Hz, 2H), 7.84 (ddd, *J* = 9.4, 7.0, 4.3 Hz, 2H), 7.73 (dt, *J* = 17.3, 8.5 Hz, 3H), 7.61 (t, *J* = 7.6 Hz, 1H), 7.46 – 7.41 (m, 2H), 7.35 (t, *J* = 7.7 Hz, 2H), 7.23 (t, *J* = 7.5 Hz, 2H), 7.16 – 7.10 (m, 4H), 7.10 – 7.04 (m, 4H), 7.01 (d, *J* = 7.8 Hz, 2H), 6.86 (t, *J* = 7.2 Hz, 1H). ¹³C NMR (100 MHz, CDCl₃) δ 147.88, 147.72, 145.76, 144.96, 141.22, 139.17, 138.62, 130.10, 130.04, 129.90, 129.69, 129.54, 128.81, 128.01, 127.72, 127.62, 127.36, 127.16, 126.86, 126.81, 126.07, 125.68, 124.72, 124.39, 123.20, 123.13, 122.98, 121.30, 120.15, 119.49, 117.08, 116.96, 109.80. HRMS (ESI, *m/z*):

[M+H]⁺ calcd for C₄₄H₃₀N₃, 600.2440; found, 600.2443.

4-(4-(14-phenyldibenzo [a, c] phenazin-9(14H)-yl) phenyl)-4H-thieno [3,2-b]indole (f): White powder; yield: 0.42 g (42%).

¹H NMR (400 MHz, CDCl₃) δ: 8.80 (dd, *J* = 8.0, 4.4 Hz, 2H), 8.31 (dd, *J* = 8.0, 1.2 Hz, 1H), 8.20 (dd, *J* = 8.1, 0.8 Hz, 1H), 7.89 – 7.79 (m, 2H), 7.79 – 7.67 (m, 4H), 7.60 (t, *J* = 7.6 Hz, 1H), 7.47 – 7.39 (m, 2H), 7.32 – 7.29 (m, 2H), 7.24 – 7.14 (m, 4H), 7.10 – 6.99 (m, 6H), 6.90 (d, *J* = 5.2 Hz, 1H), 6.84 (t, *J* = 7.0 Hz, 1H). ¹³C NMR (100 MHz, CDCl₃) δ 147.68, 147.12, 145.53, 145.27, 144.85, 141.54, 138.93, 138.37, 131.60, 130.02, 129.92, 129.57, 129.50, 129.09, 128.81, 128.28, 127.81, 127.64, 127.30, 127.15, 126.82, 126.77, 126.61, 125.96, 125.71, 125.63, 125.35, 124.71, 124.40, 123.20, 123.12, 122.71, 122.01, 121.32, 119.87, 118.83, 117.17, 117.06, 117.04, 111.40, 111.03. HRMS (ESI, *m/z*): [M+H]⁺ calcd for C₄₂H₂₈N₃S, 606.2004; found, 606.2009.

9-(4'-(9H-carbazol-9-yl)-[1,1'-biphenyl]-4-yl)-14-phenyl-9,14-dihydrodibenzo[a,c]phenazine (g): White powder, yield: 0.52 g (77%).

¹H NMR (400 MHz, CDCl₃) δ 8.77 (dd, *J* = 8.2, 3.2 Hz, 2H), 8.18 (d, *J* = 7.4 Hz, 1H), 8.13 (dd, *J* = 7.5, 4.3 Hz, 3H), 7.84 – 7.76 (m, 2H), 7.69 – 7.49 (m, 8H), 7.38 (dt, *J* = 8.9, 7.2 Hz, 8H), 7.29 – 7.26 (m, 2H), 7.05 (m, 6H), 6.80 (m, 1H). ¹³C NMR (100 MHz, CDCl₃) δ: 147.56, 147.33, 145.00, 144.48, 140.88, 140.85, 139.75, 138.37, 137.80, 136.03, 132.40, 129.99, 129.92, 129.42, 129.37, 128.85, 127.68, 127.49, 127.40, 127.35, 127.23, 127.09, 127.04, 126.65, 126.62, 125.90, 125.62, 125.42, 124.68, 124.57, 123.33, 123.12, 123.07, 121.22, 120.27, 119.85, 116.96, 116.66, 109.83. HRMS (ESI, *m/z*): [M+H]⁺ calcd for C₅₀H₃₄N₃, 676.2753; found, 676.2755.

9-phenyl-14-(4-(9-phenyl-9H-carbazol-3-yl)phenyl)-9,14-dihydrodibenzo[a,c]phenazine (h): White powder, yield: 0.56 g (83%).

¹H NMR (400 MHz, CDCl₃) δ: 8.79 (d, *J* = 8.3 Hz, 2H), 8.22 (d, *J* = 7.8 Hz, 2H), 8.15 (dd, *J* = 14.1, 7.9 Hz, 2H), 7.84 (dd, *J* = 6.8, 2.4 Hz, 1H), 7.81 (dd, *J* = 6.2, 3.0 Hz, 1H), 7.72 – 7.66 (m, 2H), 7.61 (dt, *J* = 13.5, 4.7 Hz, 6H), 7.54 – 7.46 (m, 2H), 7.45 – 7.35 (m, 7H), 7.30 (d, *J* = 3.1 Hz, 1H), 7.14 (d, *J* = 8.7 Hz, 2H), 7.11 – 7.03 (m, 4H), 6.83 (m, 1H). ¹³C NMR (100 MHz, CDCl₃) δ 147.72, 146.44, 144.79, 144.66, 141.23, 139.94, 137.98, 137.96, 137.69, 134.68, 132.96, 129.93, 129.90, 129.85, 129.46, 129.42, 129.04, 128.83, 128.23, 128.06, 127.50, 127.39, 127.35, 127.15, 127.01, 126.97, 126.51, 126.48, 125.97, 125.39, 125.32, 124.99, 124.67, 124.61, 123.75, 123.45, 123.03, 123.02, 121.08, 120.28, 119.91, 118.07, 117.36, 116.82, 109.85, 109.82. HRMS (ESI, *m/z*): [M+H]⁺ calcd for C₅₀H₃₄N₃, 676.2753; found, 676.2756.

9-phenyl-14-(4'-(1-phenyl-1H-benzo[d]imidazol-2-yl)-[1,1'-biphenyl]-4-yl)-9,14-dihydrodibenzo[a,c]phenazine (i): Yellow powder, yield: 0.25 g (35.7%).

¹H NMR (400 MHz, CDCl₃) δ: 8.78 (d, *J* = 8.3 Hz, 2H), 8.13 (dd, *J* = 8.0, 3.8 Hz, 2H), 7.89 (d, *J* = 7.9 Hz, 1H), 7.83 – 7.77 (m, 2H), 7.69 (t, *J* = 7.6 Hz, 2H), 7.57 (dd, *J* = 15.7, 8.0 Hz, 4H), 7.48 (dd, *J* = 16.2, 7.4 Hz, 3H), 7.44 – 7.32 (m, 7H), 7.30 (d, *J* = 5.5 Hz, 2H), 7.25 (d, *J* = 7.5 Hz, 2H), 7.11 – 6.98 (m, 6H), 6.80 (t, *J* = 6.6 Hz, 1H). ¹³C NMR (100 MHz, CDCl₃) δ 152.27, 149.28, 147.51, 147.29, 144.89, 144.40, 143.07, 141.37, 139.81, 138.29, 137.90, 137.71, 137.31, 137.11,

132.14, 129.97, 129.89, 129.75, 129.71, 129.39, 129.26, 129.10, 129.06, 128.83, 128.54, 128.25, 127.88, 127.46, 127.42, 127.27, 127.05, 127.02, 126.63, 126.60, 126.03, 125.58, 125.40, 125.32, 124.66, 124.53, 123.23, 123.09, 123.05, 122.95, 121.16, 119.76, 116.80, 116.77, 116.52, 110.38. HRMS (ESI, *m/z*): [M+H]⁺ calcd for C₅₁H₃₅N₃, 703.2862; found, 703.2861.

X-ray crystallography

The single crystal X-ray diffractometer data were collected at 140 K on a Rigaku RAXIS RAPID IP imaging plate system with Mo K α radiation (λ = 0.71073 Å). Single crystals suitable for X-ray crystallographic analyses were grown by slow evaporation of their respective solutions in CH₂Cl₂/n-hexane at room temperature. Important crystal data pertinent to individual compounds and the structure refinement results were assembled in ESI. The structures were solved by the direct methods, and expanded by difference Fourier syntheses using the software SHELXTL. Structure refinements were made on F² by the full-matrix least-squares technique. All nonhydrogen atoms were refined with anisotropic displacement parameters. The hydrogen atoms were placed in their ideal positions but not refined. Full crystallographic data, excluding structure factors, have been deposited at the Cambridge Crystallographic Data Center. CCDC 992518 (a), 992519 (e), 992520 (i) contain the supplementary crystallographic data for this paper. These data can be obtained free of charge from the Cambridge Crystallographic Data Centre via www.ccdc.cam.ac.uk/data_request/cif.

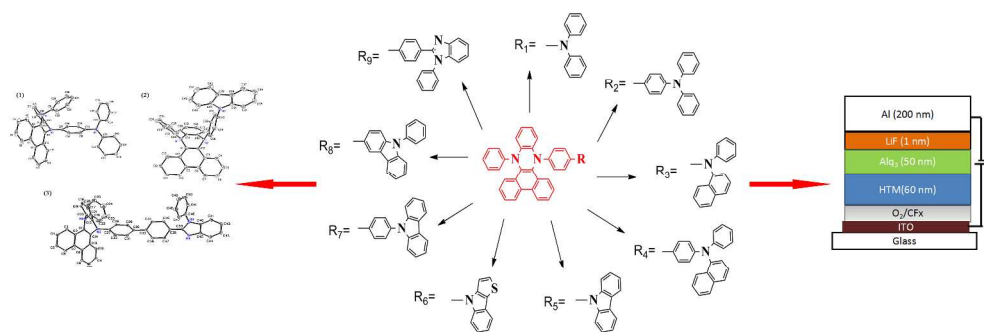
Acknowledgements

Q.Dong thanks the financial support from the National Natural Foundation of China (Grant No.: 61307030), The Natural Science Foundation for Young Scientists of Shanxi Province, China (Grant No.: 2014021019-2), and the Outstanding Young Scholars Cultivating Program and the Qualified Personal Foundation of Taiyuan University of Technology (Grant No.: 2013Y003, tyut-rc201275a).

Notes and references

- ^a Key Laboratory for Advanced Materials and Institute of Fine Chemicals, East China University of Science & Technology, Shanghai 200237, P. R. China. Fax: (86) 21-64252288; Tel: (86) 21-64252288; E-mail: huangjh@eucst.edu.cn; bbsjh@eucst.edu.cn
- ^b MOE Key Laboratory for Interface Science and Engineering in Advanced Materials and Research Center of Advanced Materials Science and Technology, Taiyuan University of Technology, 79 Yingze West Street, Taiyuan 030024, P.R. China.
- † Electronic Supplementary Information (ESI) available: [Synthetic procedure of intermediates 1-11, ¹H NMR, ¹³CNMR, mass spectrometry, optical and electrochemical, thermal properties of all the target molecules and single crystal data of selected molecules]. See DOI: 10.1039/b000000x/
- [1] (a) H. Utsumi, D. Nagahama, H. Nakano and Y. Shirota, *J. Mater. Chem.*, 2000, **10**, 2436; (b) L. S. Huang and C. H. Chen, *Mater. Sci. Eng. R*, 2002, **39**, 143; (c) F. C. Chen, T. Yang, M. E. Thompson and J. Kido, *Appl. Phys. Lett.*, 2002, **80**, 2308; (d) B. W. D'Andrade and S. R. Forrest, *Adv. Mater.*, 2004, **16**, 1585.
- [2] U. Mitschke and P. Bauerle, *J. Mater. Chem.*, 2000, **10**, 1471.
- [3] (a) B. Pan, B. Wang, Y. Wang, P. Xu, L. Wang, J. Chen, D. Ma, *J. Mater. Chem. C*, 2014, **2**, 2466-2469; (b) B. Pan, H. Huang, X. Yang, J. Jin, S. Zhuang, G. Mu, L. Wang, *J. Mater. Chem. C*, 2014, **2**, 7428-7435; (c) W. Qin, J. Liu, S. Chen, J. W. Y. Lam, M. Arseneault,

- Z. Yang, Q. Zhao, H. S. Kwok, B. Z. Tang, *J. Mater. Chem. C*, 2014, **2**, 3756-3761. (d) P. Strohrriegel and J. V. Grazulcius, *Adv. Mater.*, 2002, **14**, 1439.
- [4] C. W. Tang and S. A. VanSlyke, *Appl. Phys. Lett.*, 1987, **51**, 913.
- 5 [5] (a) J. Huang, J. H. Su and H. Tian, *J. Mater. Chem.*, 2012, **22**, 10977; (b) S. Tokito, H. Tanaka, K. Noda, A. Okada, Y. Taga, *Appl. Phys. Lett.*, 1997, **70**, 1929; (c) M. D. Joswick, I. H. Cambell, N. N. Barashkov, J. P. Ferraris, *J. Appl. Phys.*, 1996, **80**, 2883; (d) E. M. Han, L. M. Do, N. Yamamoto, M. Fujihira, *Thin Solid Films*, 1996, **273**, 202. (e) J. Y. Shen, C. Y. Lee, T. H. Huang, J. T. Lin, Y. T. Tao, C. H. Chien, *J. Mater. Chem.*, 2005, **15**, 2455.
- 10 [6] J. Huang, J. H. Su, X. Li, M. K. Lam, K. M. Fung, H. H. Fan, K. W. Cheah, C. H. Chen and H. Tian, *J. Mater. Chem.*, 2011, **21**, 2957.
- [7] (a) W. Y. Wong and C. L. Ho, *J. Mater. Chem.*, 2009, **19**, 4457; (b) M. H. Ho, M. T. Hsieh, K. H. Lin, T. M. Chen, J. F. Chen and C. H. Chen, *Appl. Phys. Lett.*, 2009, **94**, 023306; (c) M. X. Yu, J. P. Duan, C. H. Lin, C. H. Cheng and Y. T. Tao, *Chem. Mater.*, 2002, **14**, 3958.
- 15 [8] C. Adachi and K. Nagai, *Appl. Phys. Lett.*, 1995, **66**, 2679.
- [9] S. A. VanSlyke, C. H. Chen and C. W. Tang, *Appl. Phys. Lett.*, 1996, **69**(15): p. 2160.
- 20 [10] P. G. Williard and C. Sun, *J. Am. Chem. Soc.*, 1997, **119**(48), 11693.
- [11] Y. Shirota, M. Kinoshita, T. Noda, K. Okumoto, and T. Ohara, *J. Am. Chem. Soc.*, 2000, **122**(44), 11021.
- [12] H. Tanaka, S. Tokito, Y. Taga and A. Okada, *Chem. Commun.*, 1996, **18**, 2175.
- 25 [13] N. Johansson, et al. *Adv. Mater.*, 1998, **10**(14), 1136.
- [14] M. Kimura, S. Kuwano, Y. Sawaki, H. Fujikawa, K. Noda, Y. Taga and K. Takagi, *J. Mater. Chem.*, 2005, **15**, 2393.
- [15] S. Zhuang, R. Shangguan, H. Huang, G. Tu, L. Wang, X. Zhu, *Dyes Pigm.*, 2014, **101**: 93.
- 30 [16] M. Cocchi, D. Virgili, G. Giro, V. Fattori, P. Di Marco, J. Kalinowski and Y. Shirota, *Appl. Phys. Lett.*, 2002, **80**, 2401.
- [17] S. L. Lai, Q. X. Tong, M. Y. Chan, T. W. Ng, M. F. Lo, S. T. Lee and C. S. Lee, *J. Mater. Chem.*, 2011, **21**, 1206.
- 35 [18] A. Thangthong, N. Prachumrak, R. Tarsang, T. Keawin, S. Jungstittiwong, T. Sudyoasuk and V. Promarak, *J. Mater. Chem.*, 2012, **22**, 6869.
- [19] T. Okamoto, E. Terada, M. Kozaki, M. Uchida, S. Kikukawa and K. Okada, *Org. Lett.*, 2003, **5**(3), 373.
- 40 [20] B. E. Koene, D. E. Loy, M. E. Thompson, *Chem. Mater.*, 1998, **10**, 2235.
- [21] (a) J. Huang, B. Xu, M. K. Lam, K. W. Cheah, C. H. Chen and J. H. Su, *Dyes Pigm.*, 2011, **89**, 155; (b) B. E. Koene, D. E. Loy, M. E. Thompson, *Chem. Mater.*, 1998, **10**: 2235; (c) M. T. Lee, H. H. Chen, C. H. Liao, C. H. Tsai, C. H. Chen, *Appl. Phys. Lett.*, 2004, **85**, 3301.
- 45 [22] M. Aonuma, T. Oyamada, H. Sasabe, T. Miki, C. Adachi, *Appl. Phys. Lett.*, 2007, **90**(18), 183503.
- [23] Y. Park, B. Kim, C. Lee, A. Hyun, S. Jang, J. H. Lee, Y. S. Gal, T. H. Kim, K. S. Kim and J. Park, *J. Phys. Chem. C*, 2011, **115**, 4843.
- [24] Z. Zhang, B. Xu, J. Su, L. Shen, Y. Xie, H. Tian, *Angew. Chem.*, 2011, **123**, 11858.
- [25] Z. Li, Z. Wu, W. Fu, D. Wang, P. Liu, B. Jiao, X. Lei, G. Zhou, Y. Hao, *Electron. Mater. Lett.*, 2013, **9**, 655.
- 55 [26] A. Fernández-Mato, J. M. Quintela, C. Peinador, *New J. Chem.*, 2012, **36**, 1634.
- [27] H. Xu, K. Yin and W. Huang, *Chem. Eur. J.*, 2007, **13**, 10281.
- [28] J. Jin, W. Zhang, Bo. Wang, G. Mu, P. Xu, L. Wang, H. Huang, J. Chen, D. Ma. *Chem. Mater.*, 2014, **26**, 2388-2395.
- 60 [29] S. Zhuang, R. Shangguan, H. Huang, G. Tu, L. Wang, X. Zhu, *Dyes and Pigments*, 2014, 101, 93-102.



Graphical Abstract
569x213mm (300 x 300 DPI)